Revisiting flavor and *CP* violation in supersymmetric $SU(5)$ with right-handed neutrinos

Jason L. Evans,[1] Kenji Kadota,[2] and Takumi Kuwahara[2]

[1]*School of Physics, KIAS, Seoul 130-722, Korea*

[2]*Center for Theoretical Physics of the Universe, Institute for Basic Science (IBS), Daejeon 34126, Korea*

(Received 5 August 2018; published 31 October 2018)

We revisit the minimal supersymmetric $SU(5)$ grand unified theory with three right-handed neutrinos in which universality conditions for soft-supersymmetry breaking parameters are imposed at an input scale above the unification scale. If the Majorana masses for the neutrinos are around 10^{15} GeV, large mixing angles and phases in the neutrino sector lead to flavor violation and *CP* violation in the right-handed down-squark and left-handed slepton sectors. Since the observed Higgs boson mass and the proton decay constraints indicate that sfermions have masses larger than a few TeV, flavor and *CP* constraints are less restrictive. We explore the constraints on models with universal soft-supersymmetry breaking input parameters coming from proton stability, electric dipole moments, $\mu \to e\gamma$ decays, and the Higgs mass observed at the LHC. Regions compatible with all constraints can be found if nonzero *A*-terms are taken.

DOI: 10.1103/PhysRevD.98.075030

I. INTRODUCTION

The collider experiments at the Large Hadron Collider (LHC) have given stringent constraints on models beyond the standard model (SM). In the minimal supersymmetric (SUSY) extension of the SM (MSSM), squarks and gluinos are severely constrained by their absence at the LHC (see Refs. [1–3]) and by the observed Higgs mass [4].

In many models, the soft-supersymmetry breaking parameters are assumed to be universal and real at the input scale. This assumption makes it easy to avoid constraints from flavor-changing and *CP*-violating processes [such as meson oscillations, rare decays, electric dipole moments (EDMs), etc.]. For most studies, the universality conditions on the soft-supersymmetry breaking parameters are imposed at the grand unification (GUT) scale, $M_{\mathrm{GUT}} \sim 2 \times 10^{16}$ GeV, where the SM gauge couplings unify. In particular, in the constrained MSSM (CMSSM) [5,6] the universality of the scalar mass (m_0), gaugino mass ($M_{1/2}$), and trilinear coupling (A_0) are assumed at the unification scale. In this simplified model, flavor and *CP*-violating processes arise only through the Cabbibo-Kobayashi-Maskawa (CKM) matrix and are suppressed due to the smallness of the CKM matrix elements. However, there is no compelling reason to take the boundary scale of the soft-supersymmetry breaking parameters to be the GUT scale, and it is quite plausible that it is above the GUT scale (the so-called super-GUT scenarios; see Refs. [7–10]) or below the GUT scale (the so-called sub-GUT scenarios; see Refs. [11–14]). In the case of super-GUT models, the low-scale soft-supersymmetry breaking parameters are affected by which the SUSY GUT model is chosen, because of the renormalization group (RG) running between the input scale and the unification scale.

Grand unified theories based on $SU(5)$ are among the more minimal options; each generation of quarks and leptons is unified into a $\bar{\mathbf{5}} + \mathbf{10}$ representations of $SU(5)$ [15–17]. Although neutrinos are massless in the SM, nonzero neutrino masses and mixing angles have been well established by the neutrino oscillation experiments [18–20]. In the context of $SU(5)$ GUTs, tiny neutrino masses are realized by introducing a singlet fermion, the right-handed neutrinos, and relying on the type-I seesaw mechanism [21–24]. Adding right-handed neutrinos to the MSSM introduces large flavor mixing in the neutrino sector, which in turn induces large flavor-changing processes in the charged lepton sector [25–30]. For super-GUT models with right-handed neutrinos, large flavor-changing processes arise in the down-quark sector as well, due to the down-quark's interaction with color-triplet Higgs field and the right-handed neutrinos [31–39].

In this paper, we revisit the super-GUT CMSSM scenario with three right-handed neutrinos. The current best fit of the neutrino oscillation experiments has revealed that the neutrino sector has large mixing angles and most likely a large nonzero Dirac *CP* phase [18–20]. Including right-handed neutrinos in super-GUT models, the resulting flavor and CP violating effects give significant constraints on the soft-supersymmetry breaking input parameters. Although maintaining proton stability is challenging in minimal $SU(5)$ SUSY GUTs with multi-TeV scale SUSY particles [40,41], the lifetime of the proton can be pushed beyond current experimental bounds by properly choosing the additional Yukawa couplings and CP phases [10], even for multi-TeV soft SUSY masses. Here, we examine the parameter space of the boundary masses, $(m_0, M_{1/2}, A_0)$, in a super-GUT CMSSM that are compatible with the Higgs mass, flavor-changing, and CP-violating constraints. More particularly, we examine constraints from meson oscillations, lepton flavor violation (LFV), electric dipole moments, and proton decay.

Previous studies revealed that the sparticle mass spectrum could change in the presence of right-handed neutrinos, even if CMSSM boundary conditions are assumed at the GUT scale [42–44]. For right-handed neutrino Majorana masses of around 10^{15} GeV, the neutrino Yukawa couplings are $\mathcal{O}(1)$ and they contribute significantly to the renormalization group equation (RGE) of the MSSM soft-supersymmetry breaking parameters. As a result, the left-handed tau slepton can be the next-lightest supersymmetric particle (NLSP) instead of right-handed sleptons. For super-GUT boundary conditions, the soft mass for right-handed sneutrinos and down squarks are also affected by the large neutrino Yukawa couplings above the GUT scale. The effect of this added running on the MSSM soft masses is not obvious and must be investigated in detail.

This paper is organized as follows: in Sec. II, we briefly review the minimal SUSY $SU(5)$ GUT with three right-handed neutrinos and its associated soft-supersymmetry breaking parameters. We then discuss the constraints on flavor and CP violation of this model; in particular, we examine the effect of meson mixing, lepton flavor violating decays $\mu \to e\gamma$, EDMs, and proton stability. Our results are presented in Sec. IV, and finally, we summarize our work in Sec. V.

II. MODEL

First, we review the minimal SUSY $SU(5)$ GUT with three right-handed neutrinos and fix our notation.

The MSSM matter fields are contained in three $\bar{\mathbf{5}} + \mathbf{10}$ representations of $SU(5)$. The chiral multiplets Φ_i are in the $\bar{\mathbf{5}}$ representation. They are composed of the right-handed down-type quark multiplets $\bar{D}_i$ and the lepton doublets L_i, while Ψ_i is in the $\mathbf{10}$ representation and is composed of the quark doublets Q_i, the right-handed up-type quark multiplets $\bar{U}_i$, and the right-handed charged leptons $\bar{E}_i$. The right-handed neutrinos $\bar{N}_i$ are singlets of $SU(5)$. The subscript i on all fields denotes the generation. The MSSM Higgs doublets, H_u and H_d, are incorporated into the fundamental and antifundamental representations of $SU(5)$, H and $\bar{H}$, with the color-triplet Higgs superfields, H_C and $\bar{H}_C$, respectively. The $SU(5)$ gauge group is spontaneously broken by the vacuum expectation value (VEV) of the $\mathbf{24}$ Higgs multiplet Σ.

A. Superpotential

The superpotential for our model is given by

$$W = \frac{f^u_{ij}}{4}\Psi_i\Psi_j H + \sqrt{2} f^d_{ij}\Psi_i\Phi_j\bar{H} + f^\nu_{ij}\Phi_i\bar{N}_j H + \frac{1}{2}(M_R)_{ij}\bar{N}_i\bar{N}_j + W_{\rm GUT} + W_{\rm Pl}. \quad (1)$$

Here, f^u and f^d contain the MSSM Yukawa couplings, and f^ν is the neutrino Yukawa coupling. M_R is the Majorana mass matrix for the right-handed neutrinos. The $SU(5)$ indices are suppressed in Eq. (1). $W_{\rm GUT}$ represents the superpotential couplings among the Higgs fields H, $\bar{H}$, and Σ, while $W_{\rm Pl}$ contains the Planck-scale suppressed operators up to dimension 5.

The Higgs-sector superpotential is given by

$$W_{\rm GUT} = \mu_H \bar{H}H + \lambda\bar{H}\Sigma H + \frac{\mu_\Sigma}{2}{\rm Tr}\Sigma^2 + \frac{\lambda_\Sigma}{3}{\rm Tr}\Sigma^3. \quad (2)$$

The adjoint Higgs $\Sigma = \Sigma^a T^a$, where $T^a (a = 1, \ldots, 24)$ is the generator of $SU(5)$, is assumed to have a VEV of the form $\langle\Sigma\rangle = v{\rm diag}(2, 2, 2, -3, -3)$ with $v = \mu_\Sigma/\lambda_\Sigma$. After symmetry breaking, the SU(5) gauge bosons acquire masses $M_X = 5\sqrt{2}g_5 v$, where g_5 is the $SU(5)$ gauge coupling. μ_H must be fine-tuned to realize the doublet-triplet splitting, $\mu_H = 3\lambda v$, and then the color-triplet Higgs superfields obtain masses $M_{H_C} = 5\lambda v$. The color-octet and weak-triplet components of Σ get a mass $M_\Sigma = \frac{5}{2}\lambda_\Sigma v$, while the SM singlet component has a mass $M_\Sigma/5$.

The higher-dimensional operators that involve the adjoint chiral superfield Σ can play a significant role in the matching conditions at the GUT scale. The following is the superpotential containing the important operators for this work:

$$W_{\rm Pl} = \frac{c_{ij}}{M_{\rm Pl}}\Psi_i^{AC}\Sigma_A^B\Phi_{jB}\bar{H}_C + \frac{c'_{ij}}{M_{\rm Pl}}\Phi_{iA}\Sigma_B^A\bar{N}_j H^B + \frac{a_{ij}}{M_{\rm Pl}}({\rm Tr}\Sigma^2)\bar{N}_i\bar{N}_j + \frac{c}{M_{\rm Pl}}{\rm Tr}[\Sigma\mathcal{W}\mathcal{W}]. \quad (3)$$

Here, $M_{\rm Pl} = 2.4 \times 10^{18}$ GeV is the reduced Planck mass and capital letters, $A, B, C, \cdots = 1 - 5$, denote the $SU(5)$ indices. The first term is introduced in order to realize the correct matching conditions for the down-Yukawa and lepton-Yukawa couplings [45–47].[1] The second term

[1]There are other operators involving Σ, such as $\Psi_i^{AB}\Phi_{jA}\Sigma_B^C\bar{H}_C$ and $\Psi_i\Psi_j\Sigma H$. However, they only modify the Yukawa couplings with the color-triplet Higgs fields.

changes the matching conditions for f^ν, and the third term gives corrections of order $\mathcal{O}(v^2/M_{\rm Pl})$ to the Majorana mass of the right-handed neutrinos. Since we assume a right-handed Majorana mass of order 10^{15} GeV, these corrections are negligible, which is confirmed in our numerical studies. The last term in Eq. (3) involving $\mathcal{W}$, the field-strength chiral superfield of $SU(5)$, gives a finite correction to the gauge coupling matching conditions at the GUT scale.[2]

Using unitary transformations in flavor space, the MSSM superfields in the mass basis, where the Yukawa matrices for up-type quarks and charged leptons are diagonalized, are given by

$$Q_i = \begin{pmatrix} U_i \\ V_{ij} D_j \end{pmatrix}, \qquad e^{-i\varphi_{u_i}} \bar{U}_i, \qquad V_{ij} \bar{E}_j \in \Psi_i,$$

$$L_i = \begin{pmatrix} e^{-i\varphi_{d_i}} U_{ij} N_j \\ E_i \end{pmatrix}, \qquad \bar{D}_i \in \Phi_i, \tag{4}$$

and then the unphysical degrees of freedom in the Yukawa couplings and Majorana mass matrices can be removed,

$$\begin{aligned} f^u_{ij} &= f^u_i e^{i\varphi_{u_i}} \delta_{ij}, \\ f^d_{ij} &= f^d_i V^*_{ij}, \\ f^\nu_{ij} &= f^\nu_j e^{i\varphi_{d_i}} U^*_{ij}, \\ (M_R)_{ij} &= e^{i\varphi_{\nu_i}} W_{ik} (M^D_R)_k e^{2i\bar{\varphi}_{\nu_k}} W_{jk} e^{i\varphi_{\nu_j}}, \end{aligned} \tag{5}$$

where f^u_i, f^d_i, f^ν_i, and $(M^D_R)_i$ are the eigenvalues of the corresponding matrices. V is identified with the CKM matrix, and the other unitary matrices, U and W, are defined such that they contain only a single CP phase. If $(M_R)_{ij}$ is taken to be diagonal, the unitary matrix W is unity and U can then be identified with the Pontecorvo-Maki-Nakagawa-Sakata (PMNS) matrix. $\varphi_{f_i} (f = u, d, \nu)$ are additional phases present above the GUT scale and are constrained as follows, $\varphi_{f_1} + \varphi_{f_2} + \varphi_{f_3} = 0$.

The mass matrix for the left-handed neutrinos comes from the dimension-5 operator generated when the right-handed neutrinos are integrated out of Eq. (1). After electroweak symmetry breaking (EWSB), the operator gives a neutrino mass matrix of

$$(m_\nu)_{ij} = \frac{v_u^2}{2} (f^\nu M_R^{-1} f^{\nu T})_{ij}. \tag{6}$$

This mass matrix is diagonalized by the PMNS matrix $U_{\rm PMNS}$,

$$m_\nu^{\rm diag} \equiv {\rm diag}(m_1, m_2, m_3) = U^T_{\rm PMNS} m_\nu U_{\rm PMNS}, \tag{7}$$

where m_i denote the mass eigenvalues. $U_{\rm PMNS}$ is characterized by three mixing angles, θ_{12}, θ_{23}, and θ_{31}, a Dirac CP phase δ_{CP}, and a diagonal matrix containing the Majorana phases. In our study, we use the central values for the mixing angles and the Dirac CP phase found in Ref. [48],

$$\begin{aligned} &\sin^2\theta_{12} = 0.297, \qquad \sin^2\theta_{23} = 0.425, \\ &\sin^2\theta_{31} = 0.0214, \qquad \delta_{CP} = 1.38\pi. \end{aligned} \tag{8}$$

The CP-violating physics in our study depends mainly on the Dirac phase and the additional GUT-scale phases. We generally choose the GUT-scale phases to maximize the CP-odd observables and ignore the Majorana phases. We give the details of how we determine the GUT-scale phases in the next section.

We also assume a normal mass ordering for the neutrinos, and we use the central values for the mass differences of

$$m_2^2 - m_1^2 = 7.37 \times 10^{-5}\ {\rm eV}^2, \quad |\Delta m^2| = 2.56 \times 10^{-3}\ {\rm eV}^2, \tag{9}$$

with $\Delta m^2 = m_3^2 - (m_2^2 - m_1^2)/2$.

B. Soft-supersymmetry breaking parameters

In our model, the boundary conditions for the soft-supersymmetry breaking parameters are set above the GUT scale. The following is the soft-supersymmetry breaking Lagrangian in terms of $SU(5)$ multiplets,

$$\begin{aligned} -\mathcal{L}_{\rm soft} = {} & (m^2_{10})^j_i \tilde{\psi}^{*i} \tilde{\psi}_j + (m^2_{\bar{5}})^j_i \tilde{\phi}^{*i} \tilde{\phi}_j + (m^2_N)^j_i \tilde{\bar{n}}^{*i} \tilde{\bar{n}}_j + m_H^2 H^\dagger H + m^2_{\bar{H}} \bar{H}^\dagger \bar{H} + m^2_\Sigma \Sigma^\dagger \Sigma \\ & + \left(\frac{(A_{10})_{ij}}{4} \tilde{\psi}_i \tilde{\psi}_j H + \sqrt{2} (A_{\bar{5}})_{ij} \tilde{\psi}_i \tilde{\phi}_j \bar{H} + (A_N)_{ij} \tilde{\phi}_i \tilde{\bar{n}}_j H + (B_N)_{ij} \tilde{\bar{n}}_i \tilde{\bar{n}}_j + {\rm H.c.} \right) \\ & + \left(\frac{1}{2} M_5 \lambda^a \lambda^a + B_H \mu_H \bar{H} H + A_\lambda \lambda \bar{H} \Sigma H + \frac{B_\Sigma \mu_\Sigma}{2} {\rm Tr} \Sigma^2 + \frac{A_\Sigma \lambda_\Sigma}{3} {\rm Tr} \Sigma^3 + {\rm H.c.} \right). \end{aligned} \tag{10}$$

Here, $\tilde{\psi}$, $\tilde{\phi}$, and $\tilde{\bar{n}}$ are the scalar components of Ψ, Φ, and $\bar{N}$, respectively. λ^a are the $SU(5)$ gauginos, and we use the same notation for the scalar components of the Higgs superfields, i.e., H, $\bar{H}$, and Σ.

[2]If the higher-dimensional operators $({\rm Tr}\Sigma^2)^2$ and ${\rm Tr}\Sigma^4$ are included, the color octet and weak triplet's masses are split by an amount $\mathcal{O}(v^2/M_{\rm Pl})$. As long as the coefficients of these operators are not too large, they can be safely ignored.

The boundary conditions for the soft-supersymmetry breaking parameters are set at an initial scale of M_*. We impose the following universality conditions on the soft parameters at M_*,

$$
\begin{aligned}
&(m^2_{10})_i^j = (m^2_{\bar{5}})_i^j = (m^2_N)_i^j = m_0^2\delta_i^j,\\
&\quad m_H^2 = m_{\bar{H}}^2 = m_\Sigma^2 = m_0^2,\\
&(A_{10})_{ij} = A_0 f^u_{ij}, \qquad (A_{\bar{5}})_{ij} = A_0 f^d_{ij}, \qquad (A_N)_{ij} = A_0 f^\nu_{ij},\\
&\quad A_\lambda = A_\Sigma = A_0,
\end{aligned}
\tag{11}
$$

and the gaugino mass is set to be $M_5(M_*) = M_{1/2}$.

In the next subsection, we give the GUT-scale matching conditions. We use one-loop RGEs for the soft parameters from M_* to $M_{\rm GUT}$, which can be found in Refs. [49,50] for the minimal SUSY $SU(5)$ with right-handed neutrinos. During the RGE evolution, the soft-supersymmetry breaking parameters are affected by the Yukawa couplings of the SU(5) GUT theory. In particular, the large mixing angles and phases of the neutrino Yukawa matrix lead to large off-diagonal components of the soft mass matrices $m^2_{\bar{5}}$ and m^2_N. These effects result in flavor-changing and CP-violating processes, which we discuss in the next section.

C. Matching conditions at GUT scale

Here, we give the GUT scale matching conditions. We begin by discussing the matching conditions for dimensionless couplings.

We use the one-loop matching conditions for the SM gauge couplings in the $\overline{\rm DR}$ scheme.

$$
\begin{aligned}
\frac{1}{g_1^2(Q)} &= \frac{1}{g_5^2(Q)} - \frac{1}{8\pi^2}\left[-10\ln\frac{M_X}{Q} + \frac{2}{5}\ln\frac{M_{H_C}}{Q}\right] - \frac{8cv}{M_{\rm Pl}},\\
\frac{1}{g_2^2(Q)} &= \frac{1}{g_5^2(Q)} - \frac{1}{8\pi^2}\left[-6\ln\frac{M_X}{Q} + 2\ln\frac{M_\Sigma}{Q}\right] - \frac{24cv}{M_{\rm Pl}},\\
\frac{1}{g_3^2(Q)} &= \frac{1}{g_5^2(Q)} - \frac{1}{8\pi^2}\left[-4\ln\frac{M_X}{Q} + 3\ln\frac{M_\Sigma}{Q} + \ln\frac{M_{H_C}}{Q}\right]\\
&\quad + \frac{16cv}{M_{\rm Pl}}.
\end{aligned}
\tag{12}
$$

Here, g_1, g_2, and g_3 are the gauge couplings of $U(1)_Y, SU(2)_L$, and $SU(3)_C$, respectively, and Q is the renormalization scale. The term proportional to c in Eq. (12) is from the higher-dimensional operator containing $\mathcal{W}$ listed in Eq. (3) and is of order $\mathcal{O}(v/M_{\rm Pl}) \sim 10^{-2}$. Its contribution to the matching conditions is, therefore, comparable to the one-loop contributions [51]. Since the SM gauge couplings at the GUT scale can be found by renormalization group running, the matching conditions lead to constraints on the GUT scale mass spectrum and couplings [10,52],

$$
\begin{aligned}
&\frac{3}{g_2^2(Q)} - \frac{2}{g_3^2(Q)} - \frac{1}{g_1^2(Q)} = \frac{1}{2\pi^2}\frac{3}{5}\ln\frac{M_{H_C}}{Q} - 12\Delta,\\
&\frac{5}{g_1^2(Q)} - \frac{3}{g_2^2(Q)} - \frac{2}{g_3^2(Q)} = \frac{3}{2\pi^2}\ln\frac{M_X^2 M_\Sigma}{Q^3},\\
&\frac{5}{g_1^2(Q)} + \frac{3}{g_2^2(Q)} - \frac{2}{g_3^2(Q)} = \frac{6}{g_5^2(Q)} + \frac{15}{2\pi^2}\ln\frac{M_X}{Q} - 18\Delta,
\end{aligned}
\tag{13}
$$

where $\Delta = 8cv/M_{\rm Pl}$. The last expression in Eq. (13) can be used to determine the unified gauge coupling g_5.

For the case with $\Delta = 0$, M_{H_C} and $M_X^2 M_\Sigma$ are strongly constrained by the low-energy spectrum and couplings, and M_{H_C} should be around 10^{15} GeV for weak scale supersymmetry breaking. However, if Planck suppressed operators are taken into consideration, the constraint on M_{H_C} is relaxed considerably [10]. In fact, the added freedom provided by Δ allows us to treat λ and λ_Σ as free parameters, which then control the size of M_{H_C},

$$
M_{H_C} = \lambda\left(\frac{M_X^2 M_\Sigma}{g_5^2\lambda_\Sigma}\right)^{1/3}.
\tag{14}
$$

$M_X^2 M_\Sigma$ is determined by the second expression in Eq. (13). The remaining two expressions in Eq. (13) can be written in terms of $\lambda, \lambda_\Sigma, g_5$, and M_{H_C}, and so g_5 and M_{H_C} are determined by our choice of λ and λ_Σ.

We use the following tree-level matching conditions for the Yukawa couplings,

$$
\begin{aligned}
y^u_{ij}(Q) &= f^u_{ij}(Q),\\
y^d_{ij}(Q) &= f^d_{ij}(Q) + \frac{2v}{M_{\rm Pl}}c_{ij},\\
y^e_{ij}(Q) &= f^d_{ji}(Q) - \frac{3v}{M_{\rm Pl}}c_{ji},\\
y^\nu_{ij}(Q) &= f^\nu_{ij}(Q) - \frac{3v}{M_{\rm Pl}}c'_{ij},
\end{aligned}
\tag{15}
$$

where y^u, y^d, y^e, and y^ν are respectively the up-type Yukawa coupling matrix, the down-type Yukawa coupling matrix, the lepton Yukawa coupling matrix, and the neutrino Yukawa coupling matrix in the MSSM with right-handed neutrinos. c_{ij} and c'_{ij} are the coefficients of the dimension-5 operators. For simplicity, we ignore the dimension-5 operators that are irrelevant for b-τ unification. In our numerical analysis, c' is also negligible since the Majorana masses for the right-handed neutrinos are of order $\mathcal{O}(10^{15})$ GeV, so that the largest neutrino Yukawa coupling is of order $\mathcal{O}(1)$.

The matching condition for the GUT-scale Yukawa coupling matrix f_d is

$$f_d = \frac{3}{5} y_d + \frac{2}{5} y_e^T, \tag{16}$$

which is found from the second and third expressions in Eq. (15).[3] Here, the superscript T denotes the transpose of the matrix.

Next, we consider the matching conditions for the soft-supersymmetry breaking parameters. When the boundary conditions for the soft-supersymmetry breaking parameters are imposed above the GUT scale, the GUT-breaking VEV has SUSY breaking corrections and is found to be [53]

$$\langle\Sigma\rangle = [v + \mathcal{O}(M_{\rm SUSY}) + F_\Sigma \theta^2]{\rm diag}(2,2,2,-3,-3), \tag{17}$$

to leading order in a typical soft-supersymmetry breaking mass scale $M_{\rm SUSY}$, where

$$F_\Sigma = v(A_\Sigma - B_\Sigma) + \cdots. \tag{18}$$

Here, ellipses stand for the higher-order correction from soft-supersymmetry breaking parameters of order $\mathcal{O}(M_{\rm SUSY}^2)$, and thus are only relevant for the B-term matching conditions discussed below. This F term also contributes to the gaugino masses at the GUT scale via the last term in Eq. (3).

Taking into account the one-loop threshold conditions and the Planck-suppressed operator, the matching condition for gaugino masses is given by [51,54]

$$\begin{aligned}
\frac{M_1}{g_1^2} &= \frac{M_5}{g_5^2} - \frac{1}{16\pi^2}\left(10M_5 + 10A_\Sigma - 10B_\Sigma + \frac{2}{5}B_H\right) \\
&\quad + \frac{\Delta(A_\Sigma - B_\Sigma)}{2}, \\
\frac{M_2}{g_2^2} &= \frac{M_5}{g_5^2} - \frac{1}{16\pi^2}\left(6M_5 + 6A_\Sigma - 4B_\Sigma + \frac{2}{5}B_H\right) \\
&\quad + \frac{3\Delta(A_\Sigma - B_\Sigma)}{2}, \\
\frac{M_3}{g_3^2} &= \frac{M_5}{g_5^2} - \frac{1}{16\pi^2}(4M_5 + 4A_\Sigma - B_\Sigma + B_H) - \Delta(A_\Sigma - B_\Sigma),
\end{aligned} \tag{19}$$

where Δ is defined in Eq. (13). M_1, M_2, and M_3 are the gaugino masses for $U(1)_Y, SU(2)_L$, and $SU(3)_C$, respectively.

For the soft scalar mass matrices as well as the scalar-trilinear matrices, we use tree-level matching conditions,

$$\begin{aligned}
&m^2_{\tilde{Q}} = m^2_{\tilde{u}} = m^2_{\tilde{e}} = m^2_{10}, \quad m^2_{\tilde{L}} = m^2_{\tilde{d}} = m^2_{\bar{5}}, \quad m^2_{\tilde{N}_R} = m^2_N, \\
&m^2_{H_u} = m^2_H, \quad m^2_{H_d} = m^2_{\bar{H}}, \\
&(A_u)_{ij} = (A_{10})_{ij}, \quad (A_d)_{ij} = (A_e)_{ji} = (A_{\bar{5}})_{ij}, \quad (A_\nu)_{ij} = (A_N)_{ij}.
\end{aligned} \tag{20}$$

Here, $m^2_{\tilde{f}}(\tilde{f} = \tilde{Q}, \tilde{L}, \tilde{u}, \tilde{d}, \tilde{e}, \tilde{N}_R)$ denote the 3×3 soft mass matrices for the sfermions, and $A_f(f = u, d, e, \nu)$ denote the 3×3 scalar-trilinear matrices. $m^2_{H_u}$ and $m^2_{H_d}$ are soft mass parameters for the MSSM Higgs doublets, H_u and H_d, respectively.

Finally, we comment on the μ and $B\mu$ terms. The supersymmetric mass and soft-supersymmetry breaking mass terms for the MSSM Higgs doublets are determined by the EWSB conditions and are found to be

$$\begin{aligned}
|\mu|^2 &= \frac{m^2_{H_d} - m^2_{H_u}\tan^2\beta + \frac{1}{2}m_Z^2(1-\tan^2\beta) + \Delta_\mu^{(1)}}{\tan^2\beta - 1 + \Delta_\mu^{(2)}}, \\
B\mu &= -\frac{1}{2}(m^2_{H_u} + m^2_{H_d} + 2\mu^2)\sin 2\beta + \Delta_B,
\end{aligned} \tag{21}$$

where Δ_B and $\Delta_\mu^{(1,2)}$ denote loop corrections [55–57]. $\tan\beta = v_u/v_d$ is the ratio of VEVs of the MSSM Higgs doublets.

Matching conditions for the MSSM μ and $B\mu$ terms in terms of the GUT-scale μ_H and $B_H\mu_H$ are derived in Ref. [50]. These expressions, plus the reality condition on the A and B terms, lead to a nontrivial constraint on the GUT-scale soft parameters given by [10]

$$A_\Sigma^2 - \frac{\lambda_\Sigma \mu}{3\lambda}(A_\Sigma - 4A_\lambda + 4B) + \left(\frac{\lambda_\Sigma\mu}{6\lambda}\right)^2 \geq 8m^2_\Sigma, \tag{22}$$

which is applied at the GUT scale. In particular, since we consider the case with $\lambda_\Sigma \ll \lambda$, this condition simplifies to $A_\Sigma^2 \geq 8m_\Sigma^2$. This constraint may be weakened by considering nonzero CP phases for the supersymmetry breaking soft masses. However, in the results presented in Sec. IV, we examine this constraint.

III. FLAVOR AND CPV PHYSICS

In the presence of the right-handed neutrinos, the large mixing angles and CP-violating phases in the neutrino sector induce large flavor and CP violation in the MSSM soft-supersymmetry breaking parameters. Proton stability also gives strong constraints on supersymmetric grand unified theories. In this section, we discuss flavor issues in super-GUTs with right-handed neutrinos, more particularly meson oscillations, lepton flavor violating (LFV) processes, EDMs, and proton decay.

[3] In regards to the dimension-5 operators, we can estimate the values from the matching condition Eq. (15). The largest coefficient is $c_{33} = 0.04$, and the other components are much less than c_{33}.

A. Meson oscillations

The flavor and CP violations in the MSSM soft masses arise from RGE effects proportional to the off-diagonal components of f^ν. This RG running generates off-diagonal components of $m^2_{\tilde{d}}$ as the soft mass is evolved from M_* to the GUT scale. The interaction that generates this flavor and CP violation involves the colored Higgs boson and is only active above the GUT scale. An approximate expression for the off-diagonal components of $m^2_{\tilde{d}}$ is given by

$$(m^2_{\tilde{d}})_{ij} \simeq -\frac{1}{8\pi^2}[f^\nu f^{\nu\dagger}]_{ij}(3m_0^2 + A_0^2)\ln\frac{M_*}{M_{\rm GUT}}, \qquad (i \neq j).$$
$$\simeq -\frac{1}{8\pi^2}e^{i(\varphi_{d_i}-\varphi_{d_j})}U_{ik}(f^\nu_k)^2U^*_{jk}(3m_0^2 + A_0^2)\ln\frac{M_*}{M_{\rm GUT}}. \tag{23}$$

Since neutrino oscillation data indicate that there are large mixing angles and CP phases in the neutrino sector, a large hierarchy between $M_{\rm GUT}$ and the input scale for the soft mass, M_*, leads to large amounts of flavor and CP violation in the right-handed down-squark mass matrix. Flavor and CP violations are also generated in the other squark mass matrices. However, for the left-handed squark and right-handed up-squark mass matrices, the off-diagonal elements are proportional to CKM matrix elements. Because of this, the flavor and CP violations in the other mass matrices, $m^2_{\tilde{u}}$ and $m^2_{\tilde{Q}}$, are much less significant. The slepton doublets mass matrix is identical to the down-squark mass matrix at the GUT scale. However, there are additional flavor and CP-violating contributions to the slepton mass matrix from the RG evolution from $M_{\rm GUT}$ down to the scale of the right-handed neutrino masses. We discuss the associated lepton flavor issues in the next subsection. We refer to the flavor violation from the off-diagonal elements of $m^2_{\tilde{d}}$ and $m^2_{\tilde{L}}$ as the nonminimal flavor violating (NMFV) contribution.

For quark flavor violation, the strongest constraint comes from meson oscillation measurements, such as K^0-$\bar{K}^0$ oscillation. In general, the meson oscillations arise from the following four-Fermi effective Hamiltonian,

$$\mathcal{H}^{\Delta F=2}_{\rm eff} = \sum_{f=L,R}\sum_{n=1}^{3}C_{nf}Q_{nf} + \sum_{n=4}^{5}C_nQ_n, \tag{24}$$

where

$$(Q_{1R})_{ij} = \bar{d}^\alpha_{iR}\gamma_\mu d^\alpha_{jR}\bar{d}^\beta_{iR}\gamma^\mu d^\beta_{jR},$$
$$(Q_{2R})_{ij} = \bar{d}^\alpha_{iL}d^\alpha_{jR}\bar{d}^\beta_{iL}d^\beta_{jR}, \quad (Q_{3R})_{ij} = \bar{d}^\alpha_{iL}d^\beta_{jR}\bar{d}^\beta_{iL}d^\alpha_{jR},$$
$$(Q_4)_{ij} = \bar{d}^\alpha_{iL}d^\alpha_{jR}\bar{d}^\beta_{iR}d^\beta_{jL}, \quad (Q_5)_{ij} = \bar{d}^\alpha_{iL}d^\beta_{jR}\bar{d}^\beta_{iR}d^\alpha_{jL}, \tag{25}$$

with color indices α, β and flavor indices i, j, which are implicit in the effective Hamiltonian. $C_{nL,R}(n = 1,2,3)$ and $C_n(n = 4,5)$ are the corresponding Wilson coefficients. The operators $Q_{iL}(i = 1,2,3)$ are obtained from $Q_{iR}(i = 1,2,3)$ by replacing $R \leftrightarrow L$.

In regards to the SUSY contribution to meson oscillations, we use the mass insertion approximation. The expression for the relevant Wilson coefficients is [58]

$$[C_{1R}]_{ij} = -\frac{\alpha_S^2}{36m^2_{\tilde{q}}}(\Delta^{(R)}_{ij})^2[4xf_6(x) + 11\hat{f}_6(x)],$$
$$[C_4]_{ij} = -\frac{\alpha_S^2}{3m^2_{\tilde{q}}}\Delta^{(L)}_{ij}\Delta^{(R)}_{ij}[7xf_6(x) - \hat{f}_6(x)],$$
$$[C_5]_{ij} = -\frac{\alpha_S^2}{9m^2_{\tilde{q}}}\Delta^{(L)}_{ij}\Delta^{(R)}_{ij}[xf_6(x) + 5\hat{f}_6(x)], \tag{26}$$

and C_{1L} is obtained from C_{1R} with the exchange $R \leftrightarrow L$.[4] Here, $m_{\tilde{q}}$ is the averaged squark mass, $x = m^2_{\tilde{g}}/m^2_{\tilde{q}}$, and $m_{\tilde{g}}$ is the gluino mass. The mass insertion parameters $\Delta^{(L,R)}_{ij}$ are defined by

$$\Delta^{(L)}_{ij} \equiv \frac{(m^2_{\tilde{Q}})_{ij}}{m^2_{\tilde{q}}}, \qquad \Delta^{(R)}_{ij} \equiv \frac{(m^2_{\tilde{d}})_{ij}}{m^2_{\tilde{q}}}, \tag{27}$$

and $f_6(x)$ and $\hat{f}_6(x)$ are the functions arising from the loop calculations. The Wilson coefficients are computed at the sparticle mass scale. In our study, we include the two-loop QCD RGE corrections to the Wilson coefficients derived in Ref. [59], and use hadron matrix elements calculated in lattice QCD simulations. For the K_0-$\bar{K}_0$ mixing, the matrix elements are given by

$$\langle\bar{K}^0|Q_{1L,R}(Q)|K^0\rangle = \frac{1}{3}m_Kf_K^2B_1(Q),$$
$$\langle\bar{K}^0|Q_{2L,R}(Q)|K^0\rangle = -\frac{5}{24}\left(\frac{m_K}{m_s+m_d}\right)^2m_Kf_K^2B_2(Q),$$
$$\langle\bar{K}^0|Q_{3L,R}(Q)|K^0\rangle = \frac{1}{24}\left(\frac{m_K}{m_s+m_d}\right)^2m_Kf_K^2B_3(Q),$$
$$\langle\bar{K}^0|Q_4(Q)|K^0\rangle = \frac{1}{4}\left(\frac{m_K}{m_s+m_d}\right)^2m_Kf_K^2B_4(Q),$$
$$\langle\bar{K}^0|Q_5(Q)|K^0\rangle = \frac{1}{12}\left(\frac{m_K}{m_s+m_d}\right)^2m_Kf_K^2B_5(Q). \tag{28}$$

Here, m_K and f_K are the mass of kaon and the kaon decay constant, respectively. m_d and m_s are the bare masses for the strange and down quarks, respectively. $B_i(Q)(i = 1,-,5)$ are referred to as B-parameters, and are calculated in lattice simulations. The numerical values for these

[4]The other Wilson coefficients, $C_{2L,R}$ and $C_{3L,R}$, are proportional to the left-right squark mixings. Although the left-right squark mixing terms are omitted from C_4 and C_5, we have included these contributions in our numerical studies.

B-parameters are evaluated at $Q = 2$ GeV in the $\overline{\rm MS}$ scheme, with values

$$B_1(2\text{ GeV}) = 0.557, \qquad B_2(2\text{ GeV}) = 0.568,$$
$$B_3(2\text{ GeV}) = 0.847, \qquad B_4(2\text{ GeV}) = 0.984,$$
$$B_5(2\text{ GeV}) = 0.714. \tag{29}$$

Here, $B_1(2\text{ GeV})$ is the global fit value of FLAG average [60], and the central values for $B_{2\text{–}5}(2\text{ GeV})$ are found in Ref. [61]. Both of them are evaluated using $N_f = 2+1$ flavor QCD lattice simulation. In the following numerical analysis, we use the lattice results for the hadron matrix elements.

Finally, we define the K_L-K_S mass difference Δm_K and the CP-violating parameter ϵ_K as follows,

$$\Delta m_K = 2\mathrm{Re}\langle \bar{K}^0 | \mathcal{H}_{\rm eff}^{\Delta S=2} | K^0 \rangle,$$
$$\epsilon_K = \frac{1}{\sqrt{2}\Delta m_K} \mathrm{Im}\langle \bar{K}^0 | \mathcal{H}_{\rm eff}^{\Delta S=2} | K^0 \rangle. \tag{30}$$

The experimental values for these parameters are [48]

$$\Delta m_K|_{\rm exp} = (3.484 \pm 0.006) \times 10^{-12}\text{ MeV},$$
$$|\epsilon_K||_{\rm exp} = (2.228 \pm 0.011) \times 10^{-3}. \tag{31}$$

The SM value for the K_L-K_S mass difference has been calculated using lattice QCD simulation [62] and the latest SM prediction for ϵ_K is found in Ref. [63],

$$\Delta m_K|_{\rm SM} = 3.19(41)(96) \times 10^{-12}\text{ MeV},$$
$$|\epsilon_K||_{\rm SM} = 2.24(19) \times 10^{-3}. \tag{32}$$

According to Ref. [63], the SUSY contribution to $|\epsilon_K|$, denoted by $|\epsilon_K^{\rm SUSY}|$, should be less than $0.31|\epsilon_K|_{\rm SM} \simeq 0.69 \times 10^{-3}$. For the new physics contribution to Δm_K, we impose that a deviation from $\Delta m_K|_{\rm SM}$ should be within the experimental and theoretical errors. However, a previous study showed that the SUSY contribution to $\Delta m_K|_{\rm SUSY}$ in the presence of the right-handed neutrinos was much smaller than the SM value [34].

B. Lepton flavor violation processes

As mentioned in the previous subsection, significant flavor violation in the left-handed slepton sector is induced by the large neutrino mixings. The off-diagonal elements of the slepton soft mass matrix are approximately given by

$$(m_{\tilde{L}}^2)_{ij} \simeq -\frac{1}{8\pi^2} \sum_k \hat{f}_{ik}^{\nu} (\hat{f}^{\nu\dagger})_{kj} (3m_0^2 + A_0^2) \ln \frac{M_*}{(M_R^D)_k}, \quad (i \neq j). \tag{33}$$

Here, we define $\hat{f}_{ij}^{\nu} \equiv f_{ik}^{\nu} e^{-i\varphi_{\nu_k}} W_{jk}^* e^{-i\bar{\varphi}_{\nu_j}}$ in terms of the unitary matrix W, which rotates the right-handed neutrino superfields.

The LFV we consider is $\mu \to e + \gamma$. According to a recent study on the LFV processes [64], this mode places the strongest constraint on LFV processes. The latest upper limit on the branching ratio for this process is

$$\mathrm{Br}(\mu \to e\gamma) < 4.2 \times 10^{-13}, \tag{34}$$

which comes from the MEG experiment [65].

The lepton LFV processes in supersymmetric models have been discussed in Refs. [25–28]. A decay rate for $l_i \to l_j \gamma$ process is given by

$$\Gamma(l_i \to l_j \gamma) = \frac{m_{l_i}^3}{4\pi} |(C_{LL} + C_{LR})_{ji}|^2, \tag{35}$$

where m_{l_i} is the mass of the lepton l_i and C_{LL} and C_{LR} are Wilson coefficients that were derived in Refs. [27,28]. The source of the C_{LL} Wilson coefficient is the LFV elements of the soft mass matrix $m_{\tilde{L}}^2$. On the other hand, the C_{LR} Wilson coefficient is from the left-right slepton mixing matrix. To compute the LFV branching fraction, we use the average value for muon lifetime to determine the total decay rate of the muon; $\Gamma_\mu^{-1} = \tau_\mu = 2.20 \times 10^{-6}$ s [48].

C. Electric dipole moments

Other possible signals of flavor and CP violation are EDMs. As already discussed above, the flavor and CP violation of the neutrino sector in the PMNS matrix and GUT-scale phase induces flavor and CP violation in the squark and slepton mass matrices. Although the soft masses could have other sources of CP violation, we assume real soft masses at the input scale and examine the effects of the induced flavor and CP violation on EDMs.

The electron EDM can be a potential signal of this induced CP-violation in the soft-supersymmetry breaking parameters. The most recent upper bound on the electron EDM, $|d_e| \lesssim 9.3 \times 10^{-29}[e\text{ cm}]$ [66], provides the most stringent constraint on our model, as is seen below.

Although the electron EDM places the most stringent constraint on our model, we have also calculated the quark EDMs and quark chromo-EDMs (CEDMs). The EDMs and CEDMs are calculated at the SUSY scale. We include both the one-loop and two-loop contributions (see Refs. [67–69]) to the parton-level EDMs in our numerical studies; however, the bino (neutralino)-sfermion one-loop diagrams with sfermion flavor violation give the dominant contribution to the EDMs. Due to a chirality flip in the loop diagram for the dipole, the diagrams with loops containing the heavier fermions provide the dominant contribution, if flavor mixing is sufficiently large. The neutralino one-loop contribution with flavor violation to the electron EDM is approximately given by [70]

$$\frac{d_e}{e} \sim \frac{g_Y^2}{32\pi^2} \frac{m_\tau}{m_{\tilde{l}}^2} \frac{\mu M_1}{m_{\tilde{l}}^2} \mathrm{Im}[(\Delta_l^{(L)})_{13} (\Delta_l^{(R)})_{31}] f(x), \quad (36)$$

where $f(x)$ is a loop function and $x = M_1^2/m_{\tilde{l}}^2$, with $m_{\tilde{l}}$ being the averaged slepton mass. M_1 is the mass of binos and μ is the supersymmetric mass parameter for Higgsinos. The mass insertion parameters are given by

$$(\Delta_l^{(L)})_{ij} \equiv \frac{(m_{\tilde{L}}^2)_{ij}}{m_{\tilde{l}}^2}, \qquad (\Delta_l^{(R)})_{ij} \equiv \frac{(m_{\tilde{e}}^2)_{ij}}{m_{\tilde{l}}^2}. \quad (37)$$

For the hadronic EDMs, we first evaluate the quark-level EDMs at the SUSY scale. We then RG evolve the Wilson coefficients, including the mixing effects of CP-odd operators [71], down to $Q = 1$ GeV. The nucleon EDMs at the hadronic scale $Q = 1$ GeV are found from the following relation, determined by lattice simulations and QCD sum rules [72,73],

$$\begin{aligned} d_p &= 0.78 d_u - 0.20 d_d + e(-1.2\tilde{d}_u - 0.15\tilde{d}_d), \\ d_n &= -0.20 d_u + 0.78 d_d + e(0.29\tilde{d}_u + 0.59\tilde{d}_d). \end{aligned} \quad (38)$$

Here, d_p and d_n are the proton and neutron EDMs, respectively; d_q and $\tilde{d}_q$ ($q = u, d$) are the quark EDMs and CEDMs, respectively.

D. Proton decay

In supersymmetric $SU(5)$ GUTs, the dominant decay mode for the proton is controlled by the dimension-5 operators generated by color-triplet Higgs boson exchange. The $p \to K^+\bar{\nu}$ mode is the main decay mode induced by these operators, and the latest constraint on this partial decay mode is $\tau(p \to K^+\bar{\nu}) \gtrsim 6.6 \times 10^{33}$ years [74,75]. Although the other decay modes, $p \to \pi^+\bar{\nu}$ and $n \to \pi^0\bar{\nu}$, are generated by the same operators, these decay modes are suppressed by CKM mixing angles. Furthermore, the experimental bounds on these decay modes are much weaker than the $p \to K^+\bar{\nu}$ mode [10]. Therefore, we consider only the $p \to K^+\bar{\nu}$ mode in this paper. Here, we discuss the relevant aspects of proton decay for our model. For details of this calculation, see Refs. [12,76–79].

The effective Lagrangian, which controls proton decay, is found by integrating out the color-triplet Higgs boson and is given by

$$\mathcal{L}_{\mathrm{eff}}^{\Delta B=1} = C_{5L}^{ijkl} \mathcal{O}_{ijkl}^{5L} + C_{5R}^{ijkl} \mathcal{O}_{ijkl}^{5R} + \mathrm{H.c.}, \quad (39)$$

with

$$\begin{aligned} \mathcal{O}_{ijkl}^{5L} &\equiv \int d^2\theta \frac{1}{2} \epsilon_{\alpha\beta\gamma} (Q_i^\alpha Q_j^\beta)(Q_k^\gamma L_l), \\ \mathcal{O}_{ijkl}^{5R} &\equiv \int d^2\theta \epsilon^{\alpha\beta\gamma} \bar{U}_{i\alpha} \bar{E}_j \bar{U}_{k\beta} \bar{D}_{l\gamma}, \end{aligned} \quad (40)$$

where parentheses denote contractions of $SU(2)_L$ indices. The greek letters represent $SU(3)_C$ indices, i, j, k, l represent the generations, and $\epsilon^{\alpha\beta\gamma}$ is the totally antisymmetric tensor. In the mass basis for the MSSM chiral multiplets, the Wilson coefficients at the GUT scale are given by

$$\begin{aligned} C_{5L}^{ijkl} &= -\frac{1}{M_{H_C}} f_i^u e^{i\varphi_{u_i}} \delta^{ij} V_{kl}^* f_l^d, \\ C_{5R}^{ijkl} &= -\frac{1}{M_{H_C}} f_i^u V_{ij} V_{kl}^* f_l^d e^{-i\varphi_{u_k}}. \end{aligned} \quad (41)$$

Here, V_{ij} is the CKM matrix, and φ_{u_i} are the additional phases in the up-type GUT Yukawa matrix f^u.

We determine the proton lifetime by first one-loop RG running the Wilson coefficients C_{5L} and C_{5R} down to the SUSY scale. The RGEs for these Wilson coefficients, found in Ref. [80], are modified in the presences of right-handed neutrinos to become

$$\beta_{5L}^{ijkl} \equiv \mu \frac{\mathrm{d}}{\mathrm{d}\mu} C_{5L}^{ijkl} = \beta_{5L;\mathrm{MSSM}}^{ijkl} + \frac{1}{16\pi^2} (y^\nu y^{\nu\dagger})_{lm} C_{5L}^{ijkm}, \quad (42)$$

where $\beta_{5L;\mathrm{MSSM}}^{ijkl}$ denotes the MSSM contribution to the RGE for C_{5L}^{ijkl} [80], and y^ν is the neutrino Yukawa matrix. Above the right-handed neutrino mass scale β_{5L}^{ijkl} is used in the RGEs and $\beta_{5L;\mathrm{MSSM}}^{ijkl}$ is used below the right-handed neutrino mass scale. At the SUSY scale, the sfermions in the effective operators in Eq. (40) are integrated out via charged wino and Higgsino exchange processes, giving the four-fermion interactions leading to proton decay. The large flavor violation in the right-handed down-squark sector does not significantly induce the other modes, such as $p \to \pi^0\mu^+$ [78].

Since the SUSY scale is a bit higher than the electroweak (EW) scale, we use the SM RGEs to evolve the coefficients from the SUSY scale to the EW scale [81]. Below the EW scale, we evolve the coefficients using the two-loop long-distance corrections [82] to obtain the coefficients at the hadronic scale. The hadron matrix elements are then evaluated at the hadronic scale using lattice simulation [83],

$$\begin{aligned} \langle K^+ | (us)_R d_L | p \rangle &= -0.049\ \mathrm{GeV}^2, \\ \langle K^+ | (us)_L d_L | p \rangle &= 0.041\ \mathrm{GeV}^2, \\ \langle K^+ | (ud)_R s_L | p \rangle &= -0.134\ \mathrm{GeV}^2, \\ \langle K^+ | (ud)_L s_R | p \rangle &= 0.139\ \mathrm{GeV}^2. \end{aligned} \quad (43)$$

IV. RESULTS

Before showing our results, we define our parameters. The GUT scale, M_{GUT}, is defined as the scale where

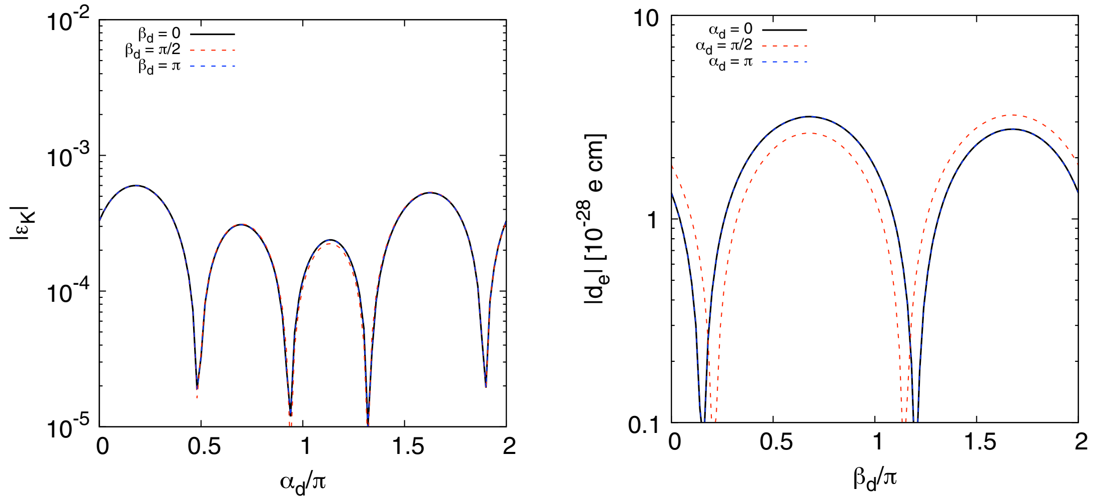

FIG. 1. GUT-scale phase dependence of $|\epsilon_K|$ and d_e. Different lines correspond to different parameter choices. $\tan\beta = 6$, $M_{1/2} = 1$ TeV, $A_0 = 0$, $\mu > 0$, and $M_* = M_{\rm Pl}$ are assumed. $|\epsilon_K^{\rm SUSY}|$ is maximized at $\alpha_d = 0.18\pi$, and $|d_e|$ is maximized at $\beta_d = 0.68\pi$.

the condition $g_1(M_{\rm GUT}) = g_2(M_{\rm GUT})$ is satisfied. The unified coupling g_5 at $M_{\rm GUT}$ is then determined using the third relation in Eq. (13). The SUSY scale is defined as the geometric mean of the stop mass eigenvalues, $M_{\rm SUSY} = \sqrt{m_{\tilde{t}_1} m_{\tilde{t}_2}}$. To ensure longevity of the proton, we also take the GUT-scale Yukawa couplings to be $\lambda(M_{\rm GUT}) = 0.5$ and $\lambda_\Sigma(M_{\rm GUT}) = 10^{-4}$ [10].

The input parameters of our model are then

$$m_0^2, \quad M_{1/2}, \quad A_0, \quad \tan\beta, \quad {\rm sgn}(\mu), \quad M_*, \quad (M_R)_{ij}, \quad \varphi_{u_i}, \quad \varphi_{d_i}, \quad \varphi_{\nu_i}, \quad \bar{\varphi}_{\nu_i}, \qquad (44)$$

after fixing λ and λ_Σ. For simplicity, we assume the right-handed neutrino mass matrix is proportional to unity, $(M_R)_{ij} = M_{N_R}\delta_{ij}$, and is real. Consequently, we find $\bar{\varphi}_{\nu_1} = \bar{\varphi}_{\nu_2} = \bar{\varphi}_{\nu_3} = 0$ and $\varphi_{\nu_1} = \varphi_{\nu_2} = \varphi_{\nu_3} = 0$. The input scale for the soft-supersymmetry breaking parameters, M_*, is set to the reduced Planck mass $M_{\rm Pl} = 2.4 \times 10^{18}$ GeV. This is because we want to determine what the most stringent constraints possible are from the flavor and *CP* violation of the neutrino sector.

The GUT-scale phases φ_u are chosen to maximize the lifetime of the proton. This allows us to focus on the constraints coming from flavor and *CP* violation. However, even with this maximization procedure, $\tan\beta \lesssim 6$ is required to get a sufficiently long proton lifetime. We take $\tan\beta = 6$ for our study. The remaining phases, φ_d, are determined by maximizing $|\epsilon_K^{\rm SUSY}|$ and the electron EDM.

Because the phases are constrained, $\varphi_{d_1} + \varphi_{d_2} + \varphi_{d_3} = 0$, there are only two independent phases, which we denote by $\alpha_d \equiv \varphi_{d_1} - \varphi_{d_2}$ and $\beta_d \equiv \varphi_{d_1} - \varphi_{d_3}$. ϵ_K is most strongly dependent on $(m_{\tilde{d}}^2)_{12}$ and α_d. α_d is then determined by maximizing ϵ_K.

In the left panel of Fig. 1, we show the α_d-dependence of $|\epsilon_K^{\rm SUSY}|$ with $M_{N_R} = 10^{15}$ GeV. We set the initial values of the soft-supersymmetry breaking parameters to be $M_{1/2} = 1$ TeV, $m_0 = 1$ TeV, $A_0 = 0$, $\tan\beta = 6$, and ${\rm sign}(\mu) > 0$. Because C_{1R} defined in Eq. (26) is proportional to $(m_{\tilde{d}}^2)_{12}^2$, four peaks appear in the plot for $|\epsilon_K|$. Since the flavor and *CP* violation in the left-handed squark sector is so much smaller than that in the right-handed sector, the $|\epsilon_K^{\rm SUSY}|$ is almost completely controlled by the NMFV contribution to the right-handed squark sector. The positions of the peaks are determined by the *CP* violation in the neutrino sector and are, therefore, mostly independent of the initial values of the soft-supersymmetry breaking parameters. In the left panel of Fig. 1, we also show $|\epsilon_K^{\rm SUSY}|$ for different values of β_d. As is seen in the figure, $|\epsilon_K^{\rm SUSY}|$ is almost completely independent of β_d. The maximum value for $|\epsilon_K^{\rm SUSY}|$ is found for $\alpha_d \simeq 0.18\pi$.

As mentioned in the previous section, the dominant contribution to the electron EDM is from the neutralino-stau loop diagram. This dominant contribution is proportional to $(m_{\tilde{L}}^2)_{13}$, and is therefore controlled by β_d. In the right panel of Fig. 1, we show the β_d-dependence of d_e, with the same input values for the soft-supersymmetry breaking parameters as the left panel. As is clear from the right panel of Fig. 1, d_e is only weakly dependent on α_d and is maximized for $\beta_d \simeq 0.68\pi$. Although d_e is only weakly dependent on α_d, this phase can be important in regions with huge cancellations. For instance, the two-loop stop-associated Barr-Zee contribution has a different *CP* phase dependence and can, therefore, have the opposite sign of

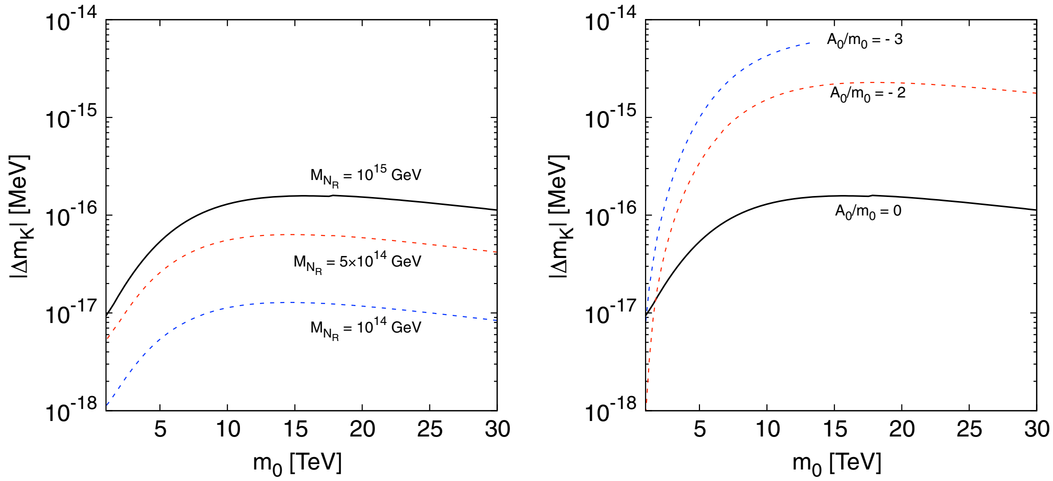

FIG. 2. SUSY contribution to kaon mass difference $|\Delta m_K|_{\mathrm{SUSY}}$ as a function of m_0. $\tan\beta = 6$, $M_{1/2} = 5$ TeV, $\mu > 0$, and $M_* = M_{\mathrm{Pl}}$ are assumed. $A_0 = 0$ in the left panel, while universal right-handed neutrino mass M_{N_R} is fixed to be 10^{15} GeV in the right panel.

the one-loop contribution. In some of the figures below, we see that the cancellation between these two contributions can be important.

Before we show the m_0-$M_{1/2}$ and m_0-A_0 planes of this model, we consider the dependence of Δm_K, the kaon mass difference, on the SUSY breaking parameters. The mass difference Δm_K can be decomposed into two pieces, $\Delta m_K = \Delta m_K|_{\mathrm{SM}} + \Delta m_K|_{\mathrm{SUSY}}$, with $\Delta m_K|_{\mathrm{SM}}$ corresponding to the SM value Eq. (32). The SUSY contribution, $\Delta m_K|_{\mathrm{SUSY}}$, should not be larger than the experimental and the theoretical uncertainties. Fig. 2 shows the m_0-dependence of $\Delta m_K|_{\mathrm{SUSY}}$ for various parameter choices of A_0 and M_{N_R} as a function of m_0. For small m_0, the SUSY contribution to Δm_K is suppressed because the dominant contribution to the squark mass is from the gaugino radiative correction.

For the left panel in Fig. 2, we vary the universal Majorana neutrino mass as $M_{N_R} = 10^{15}, 5\times10^{14}$, and 10^{14} GeV from top to bottom, with fixed $A_0 = 0$. The M_{N_R} dependence of $|\Delta m_K|$ is explained by the neutrino Yukawa dependence on M_{N_R}. The SUSY contribution to $|\Delta m_K|$ is largest for large M_{N_R}, because the neutrino Yukawa couplings are larger leading to more flavor violation.

In the right panel of Fig. 2, we show the A_0-dependence of $\Delta m_K|_{\mathrm{SUSY}}$ for $M_{N_R} = 10^{15}$ GeV. The flavor violation in the down-squark sector induced by RGE running from M_* to M_{GUT} has a piece proportional to an A-term. This dependence leads to the growth of $|\Delta m_K|$ as $|A_0/m_0|$ is increased. However, if the A-terms are taken too large, some of the sfermions become tachyonic. This is seen in Fig. 2 by the fact that the line with $A_0/m_0 = -3$ terminates for $m_0 \sim 13$ TeV.

Examining both panels of Fig. 2, we see that the SUSY contribution to the kaon mass difference is less than $\mathcal{O}(1)\%$. Although $\Delta m_K|_{\mathrm{SUSY}}$ is much smaller than the SM predictions, we include it since it is important for calculating $\epsilon_K^{\mathrm{SUSY}}$ in what follows.

The level of precision and method used to calculate the SUSY spectrum is as follows. For the soft-supersymmetry breaking parameters we use the one-loop RGEs between M_* and the GUT scale and the matching conditions discussed in Sec. II are used at the GUT scale. The RGEs for the soft masses of scalars and gauginos below the GUT scale are at the two-loop level and the other parameters are at the one-loop level. We, of course, take into account the complex phases and the off-diagonal flavor mixing parts of the RGEs, since our focus is on flavor and CP violation. The mass spectrum and mixing matrices for the Higgs boson, sfermions, neutralinos, and charginos are evaluated using `FeynHiggs 2.14.2`.

Now, in Fig. 3 we show the m_0-$M_{1/2}$ plane with $M_* = M_{\mathrm{Pl}}$, $M_{N_R} = 10^{15}$ GeV, and $\tan\beta = 6$. The difference between the left and right panels is just the sign of the μ-parameter; positive (negative) μ is used in the right (left) panels. We set different values for A_0/m_0 in the top and bottom panels; $A_0 = 0(-3m_0)$ is assumed in the top (bottom) panels. In each figure, we have plotted the Higgs mass contours (green dotted-lines), proton decay constraints (black lines), $|\epsilon_K^{\mathrm{SUSY}}|$ contours (red-brown lines), future prospect for the electron EDM ($\sim 10^{-31}$ e cm shown by the red-dashed lines), and the MEG-II sensitivity to $\mu \to e\gamma$ decays ($\mathrm{Br}(\mu\to e\gamma) \sim 6\times10^{-14}$ [84] shown by the yellow-dashed line). In the purple shaded region, the mass difference between the lightest neutralino and stop, $m_{\tilde{t}_1} - m_{\chi_1^0}$, is less than 100 GeV.[5] The other shaded regions in Fig. 3 are excluded because the electron EDM is larger

[5]Since the bino mass for the entire purple region is less than about 3 TeV and the A-terms are large, some of the purple shaded region should have a viable dark matter candidate due to coannihilation of the bino with the stop [11,85].

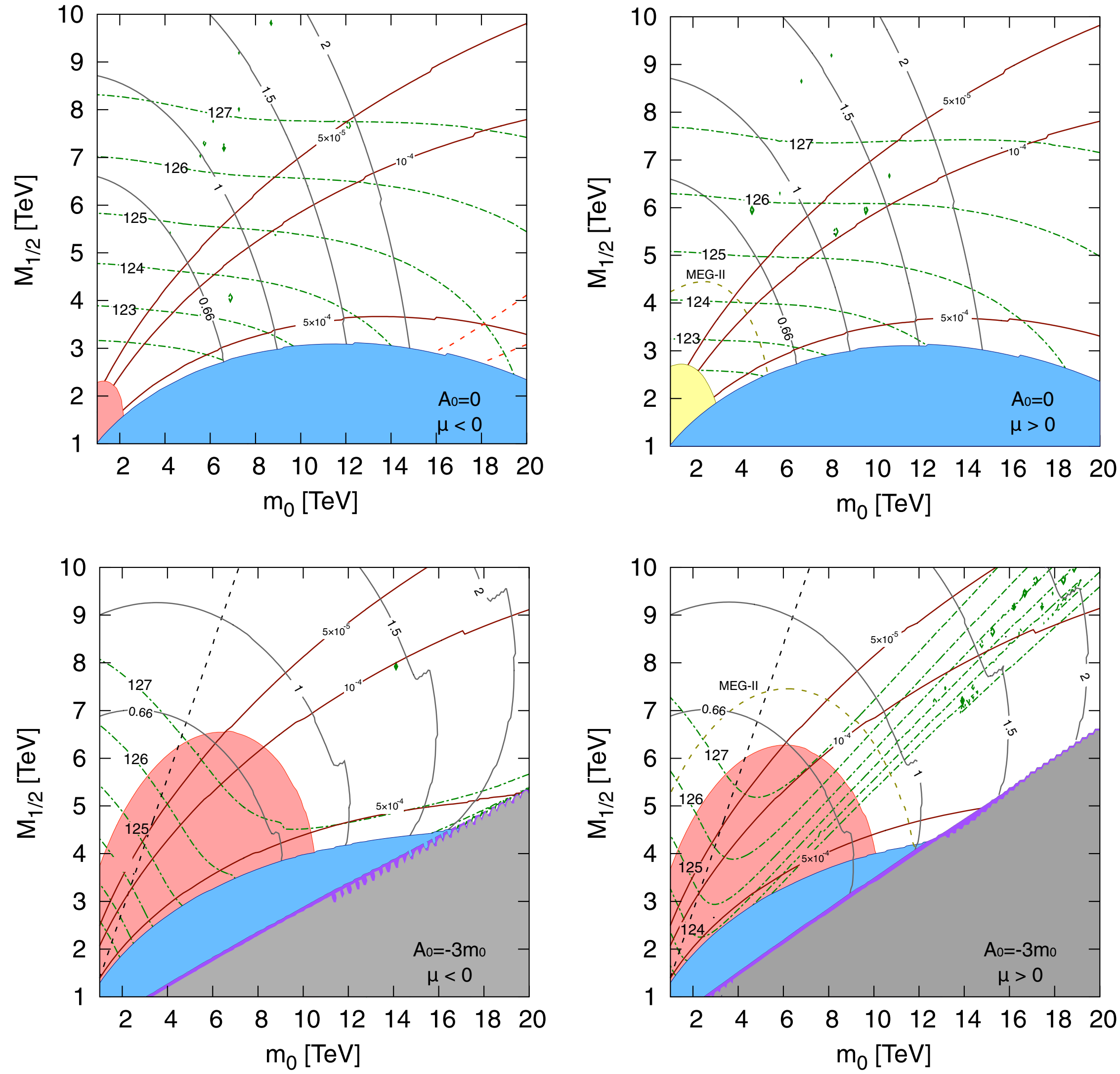

FIG. 3. The m_0-$M_{1/2}$ plane for $\tan\beta = 6$, $M_* = M_{\rm Pl}$, $M_{N_R} = 10^{15}$ GeV, and $\mu < 0$ ($\mu > 0$) in the left (right) panels. $A_0 = 0(-3m_0)$ is assumed in the top (bottom) panels. The red-brown lines show the SUSY contribution to $|\epsilon_K|$, with the contribution exceeding 0.69×10^{-3} in the cyan-shaded region. The black-solid lines indicate the partial proton lifetime $\tau(p \to K^+\bar{\nu})$ in units of 10^{34} years. The green dotted lines illustrate the mass of the light Higgs boson. The red and yellow-shaded regions are excluded by the current electron EDM and $\mu \to e\gamma$ bound, respectively. The mass difference $m_{\tilde{\tau}_1} - m_{\chi_1^0}$ is below 100 GeV in the purple shaded region.

than 9.3×10^{-29} $[e\,{\rm cm}]$ (the red region), the branching fraction for $\mu \to e\gamma$ is larger than 4.2×10^{-13} (the yellow region), or $|\epsilon_K^{\rm SUSY}|$ exceeds 0.69×10^{-3} (the cyan region). Even though we have checked the nucleon EDMs in this paper, the constraints are much weaker than the constraints presented. According to `FeynHiggs 2.14.2`, the SUSY contribution to the ${\rm Br}(B \to X_s\gamma)$ is less than 1% of the SM prediction, and therefore can be ignored.

Since off-diagonal components of soft masses are proportional to m_0^2 and A_0^2 [Eqs. (23) and (33)], no flavor and *CP* violation is generated if m_0 vanishes at the input scale. The flavor and *CP* violation is maximized when sfermion masses are dominated by m_0^2 not $M_{1/2}$, and then the violation decreases when sfermions are decoupled. Therefore, the flavor and *CP*-violating observables have a peak along m_0 axis for fixed $M_{1/2}$.

In the top panels of Fig. 3, the LSP is a binolike neutralino throughout the entire plane. The RGE running of the soft-supersymmetry breaking parameters above the GUT scale lifts the mass of all charged scalars above the neutralino mass. Because of the right-handed neutrinos, the mass spectrum at the GUT scale is altered. Without the right-handed neutrino, the lightest sfermion mass is $(m_{10}^2)_3^3$, due to RG running effects of the top Yukawa coupling. However, the neutrino Yukawa couplings suppress the mass of Φ_3 leading to $(m_{10}^2)_3^3 > (m_{\bar{5}}^2)_3^3$.

In our setup, due to the large Yukawa couplings for the neutrinos and the large group-theoretic numerical factors of

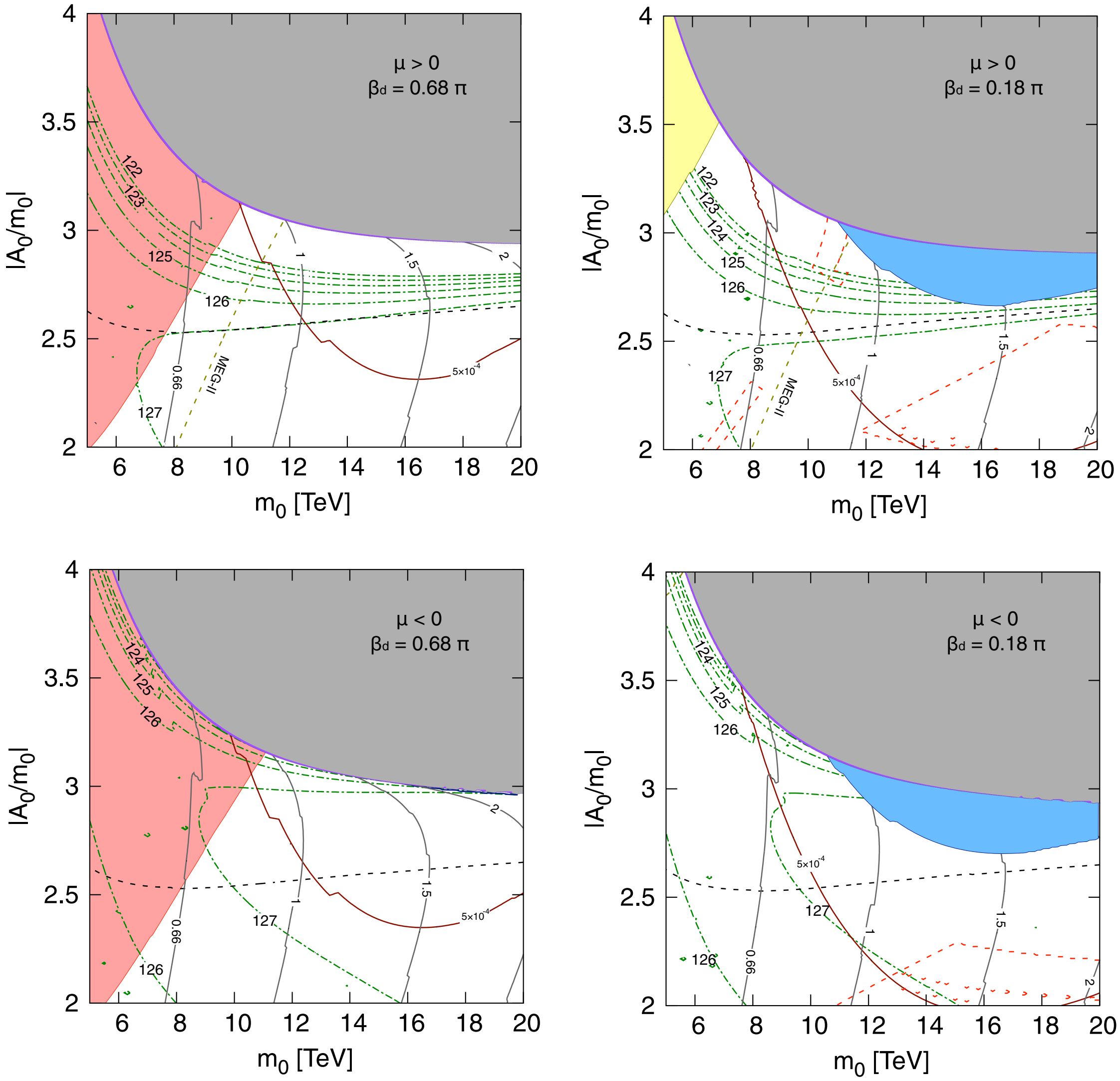

FIG. 4. $m_0 - A_0/m_0$ contour plots. $M_{1/2} = 4.5$ TeV, and $\tan\beta = 6$ are assumed. Black-solid lines indicate the partial proton lifetime $\tau(p \to K^+\bar{\nu})$ in units of 10^{34} years. Black-shaded regions are excluded by the charge-color breaking (CCB)-charged/colored LSP (CLSP) constraints. Above the black-broken lines the B-condition is satisfied. The green dotted lines indicate the Higgs mass. The mass difference $m_{\tilde{t}_1} - m_{\chi_1^0}$ is below 100 GeV in the purple shaded region. The red and yellow shaded regions are excluded by the current bounds, and the red and yellow dashed lines are future limits from the electron EDM and $\mu \to e\gamma$, respectively.

SU(5), the diagonal components of m_N^2, the soft-mass matrix for the right-handed neutrinos, is driven negative by RGE effects. A positive m_N^2 drives $m_{\bar{5}}^2$ to smaller values, as seen in Refs. [42–44]. However, because m_N^2 promptly turns negative, the mass of $m_{\bar{5}}^2$ is not so suppressed.

The sign of μ affects flavor and CP-violating processes involving left-right sfermion mixing. This dependence is rather important when the final result involves a cancellation. In particular, the neutralino one-loop contribution to the electron EDM cancels with the stop-associated Barr-Zee contribution for $\mu < 0$. This cancellation leads to the weaker electron EDM constraint in the left panel of Fig. 3, for small m_0 and $M_{1/2}$. This region is instead excluded by the $\mu \to e\gamma$ bounds. The LFV constraints in this region are enhanced for sign$(\mu) > 0$, since the Wilson coefficients C_{LL} and C_{LR} in Eq. (35) have the right signs to add.

The B matching condition in Eq. (22) cannot be satisfied[6] for $A_0 = 0$ over the entire plane. To satisfy the B matching condition, we now consider nonzero A-terms. Nonzero input values for A_0 enhance flavor violation as shown in Eqs. (23) and (33).

To satisfy the B matching condition, we take the same parameters used in the top panels of Fig. 3, except $A_0 = -3m_0$, and plot the m_0-$M_{1/2}$ plane in the bottom panels of Fig. 3. The larger A-term enhances the LFV in the lepton sector leading to a much larger region excluded by

[6]If the A-terms are complex, this condition may be weakened.

electron EDM constraints, the red region. The mass difference of the lightest stop and neutralino is below 100 GeV in the purple region, and the gray region with larger m_0 is excluded due to a tachyonic stop.[7] Below the black dashed line in the bottom panels, the B matching condition is satisfied.

In Fig. 4, we show $m_0 - A_0/m_0$ contour plots with the boundary gaugino mass taken to be $M_{1/2} = 4.5$ TeV and $\tan\beta = 6$. We choose $\beta_d = 0.68\pi$, the maximal value for the phase controlling the electron EDM, in the left figure and a more moderate value of $\beta_d = 0.18\pi$ for the right figure. We assume positive (negative) μ in the top (bottom) panels of Fig. 4. The B matching condition is satisfied above the black dashed lines in each panel. The gray-shaded regions are excluded because the LSP is colored/charged or it has a CCB minimum due to tachyonic charged sfermion. We will refer to this region as the CCB-CLSP constraints.

The current bound for the electron EDM, $|d_e| < 9.3 \times 10^{-29}$ [e cm] [66], puts the strongest constraint on the parameter space for the figures with $\beta_d = 0.68\pi$. In the right panels, the electron EDM constraints are weaker. However, the future sensitivity of the ACME experiment can put rather severe constraints on this parameter space. Most of the parameter space is accessible to the ACME experiments, with the sensitivity indicated by the red-dashed line. For the left two figures of Fig. 4, the entire parameter space is in reach of the ACME experiments. The right two figures have some blind spots. Because of cancellations among the one-loop and two-loop contributions to the electron EDMs for $\mu > 0$, the prediction is beyond the future sensitivity of ACME for the islands around $m_0 \simeq 6$–10 TeV.

Although the EDM constraints become weaker in the figures with $\beta_d = 0.18\pi$, the LFV muon decay still constrains the parameters space, if the Higgsino mass parameter μ is assume to be positive. In particular, the expected future sensitivity at the MEG-II experiment, $\mathrm{Br}(\mu \to e\gamma) \simeq 6 \times 10^{-14}$ [84], will be comparable to the current proton decay constraint.

The future sensitivity of the Hyper-Kamiokande experiment to proton decay is reported as $\tau(p \to K^+\bar{\nu}) \simeq 2.5 \times 10^{34}$ years at 90% confidence level [86]. Thus, the whole parameter space shown in Fig. 4 will be tested by future proton decay experiments.

Lastly, we give the mass spectrum for a reference point in Table I for a point near the CCB-CLSP boundary in the left-bottom panel of Fig. 4. In the case of minimal $SU(5)$, it is hard to observe squarks with a mass above 10 TeV, even at high-energy colliders with $\sqrt{s} = 100$ TeV.[8] In contrast to models with CMSSM matter content, minimal SU(5) super-GUTs with right-handed neutrinos, and a large neutrino Yukawa matrix, break the degeneracy of the first two generation sfermions. If this degeneracy is sufficiently broken, the effects of the first and second generation sfermions may be detectable at future experiments.

TABLE I. Sparticle and Higgs mass spectrum.

Input	
m_0	15.1 [TeV]
$M_{1/2}$	4.5 [TeV]
A_0/m_0	−3.02
$\tan\beta$	6
sign(μ)	−1

Particle	Mass
h	125.2 [GeV]
$H, A, H^\pm$	23.0 [TeV]
$(\chi_1^0, \chi_2^0, \chi_3^0, \chi_4^0)$	(2.56, 4.14, 19.2, 19.2) [TeV]
$(\chi_1^\pm, \chi_2^\pm)$	(4.14,19.2) [TeV]
$\tilde{g}$	8.70 [TeV]
$(\tilde{\nu}_1, \tilde{\nu}_2, \tilde{\nu}_3)$	(12.6,12.8,15.0) [TeV]
$(\tilde{\tau}_1, \tilde{\tau}_2)$	(10.4,13.1) [TeV]
$(\tilde{e}_{L1}, \tilde{e}_{L2}, \tilde{e}_{R1,2})$	(14.2,15.4,16.1) [TeV]
$(\tilde{t}_1, \tilde{t}_2)$	(2.61,10.9) [TeV]
$(\tilde{b}_1, \tilde{b}_2)$	(10.9,12.6) [TeV]
$(\tilde{u}_L, \tilde{u}_R)$	(16.8,17.3) [TeV]
$(\tilde{d}_{R1}, \tilde{d}_{R2}, \tilde{d}_{L1,2})$	(15.9,17.0,17.3) [TeV]

V. CONCLUSION

In this work, we have revisited the minimal supersymmetric $SU(5)$ with three right-handed neutrinos. Using the best-fit values for the neutrino mixing angles, the Dirac phase, and the SM parameters, we evaluated the low-scale sparticle mass spectrum using CMSSM-like input masses and calculated the relevant flavor and *CP*-violating signatures.

We have focused on the case with right-handed neutrinos masses around 10^{15} GeV. The large neutrino Yukawa couplings, large mixing angles, and *CP* phase for this case induce significant flavor-changing and *CP*-violating processes. Kaon mixing, the electron EDM, and proton decay are the most important constraints on this model. The other important experimental constraint, the Higgs mass with $m_h \simeq 125$ GeV, is compatible with the flavor and *CP*-violating constraints if the A-terms are large at the boundary scale. Although the strongest constraints are currently from proton decay, future experiments, such as MEG-II and

[7]Although we do not calculate it, along this boundary there is a region where stop coannihilation can occur. Since the region excluded by the electron EDM and kaon oscillation constraints only extends to $M_{1/2} \sim 4$ TeV, bino dark matter from stop coannihilation extends well beyond the constraints [11,85].

[8]Gluinos with a mass below 10 TeV can potentially be discovered at a 100 TeV colliders [87].

ACME experiments, will probe some of the parameter space of these models in a complementary way.

Because of the presences of right-handed neutrinos, there are more GUT-scale phases than in minimal $SU(5)$. Because these phases are not restricted by low-energy physics, they are, in general, free parameters. Some of these phases, φ_{u_i}, are used to suppress proton decay, while others, φ_{d_i}, are taken to maximize CP violation for the most stringent bounds. This work focused on the effects of GUT-scale phases on flavor and CP violation. However, the CP-odd observables also depend on a CP phase in the soft-supersymmetry breaking parameters, which we have set to 0. These additional phases could lead to cancellations in the contributions to CP-odd observables. We also note that we assumed the normal hierarchical structure for the neutrino masses and a diagonal mass matrix for the right-handed neutrinos. The constraints from flavor and CP observables are expected to change by a factor of 2 if the inverted hierarchy is assumed. The flavor and CP constraints can also change if we take a more generic flavor structure for the right-handed neutrino sector.

Concerning the mass spectrum in the presence of the right-handed neutrinos, the previous studies with CMSSM boundary masses have revealed that the left-handed stau can be the NLSP instead of the right-handed stau. Contrary to what we expected, this is not possible in super-GUT models with right-handed neutrinos due to radiative corrections involving GUT-scale particles and the right-handed neutrinos. These corrections drive the neutrino soft mass negative above the GUT scale. The radiative corrections below the GUT scale then have the opposite effect.

Although almost all sparticles are too heavy to be discovered at collider experiments, intensity-frontier experiments can potentially discover and/or constrain these models.

ACKNOWLEDGMENTS

We thank K. A. Olive for useful discussion. The work of K. K. and T. K. was supported by IBS under Grant No. IBS-R018-D1.

[1] G. Aad *et al.* (ATLAS Collaboration), Summary of the searches for squarks and gluinos using $\sqrt{s} = 8$ TeV pp collisions with the ATLAS experiment at the LHC, J. High Energy Phys. 10 (2015) 054.

[2] M. Aaboud *et al.* (ATLAS Collaboration), Search for squarks and gluinos in final states with jets and missing transverse momentum using 36 fb^{-1} of $\sqrt{s} = 13$ TeV pp collision data with the ATLAS detector, Phys. Rev. D **97**, 112001 (2018).

[3] A. M. Sirunyan *et al.* (CMS Collaboration), Search for Physics Beyond the Standard Model in Events with High-Momentum Higgs Bosons and Missing Transverse Momentum in Proton-Proton Collisions at 13 TeV, Phys. Rev. Lett. **120**, 241801 (2018).

[4] G. Aad *et al.* (ATLAS and CMS Collaboration), Combined Measurement of the Higgs Boson Mass in pp Collisions at $\sqrt{s} = 7$ and 8 TeV with the ATLAS and CMS Experiments, Phys. Rev. Lett. **114**, 191803 (2015).

[5] H. P. Nilles, Supersymmetry, supergravity and particle physics, Phys. Rep. **110**, 1 (1984).

[6] G. L. Kane, C. F. Kolda, L. Roszkowski, and J. D. Wells, Study of constrained minimal supersymmetry, Phys. Rev. D **49**, 6173 (1994).

[7] J. Ellis, A. Mustafayev, and K. A. Olive, Resurrecting no-scale supergravity phenomenology, Eur. Phys. J. C **69**, 219 (2010).

[8] J. Ellis, A. Mustafayev, and K. A. Olive, What if supersymmetry breaking unifies beyond the GUT scale?, Eur. Phys. J. C **69**, 201 (2010).

[9] E. Dudas, Y. Mambrini, A. Mustafayev, and K. A. Olive, Relating the CMSSM and SUGRA models with GUT scale and super-GUT scale supersymmetry breaking, Eur. Phys. J. C **72**, 2138 (2012); Erratum, Eur. Phys. J. C **73**, 2430(E) (2013).

[10] J. Ellis, J. L. Evans, A. Mustafayev, N. Nagata, and K. A. Olive, The super-GUT CMSSM revisited, Eur. Phys. J. C **76**, 592 (2016).

[11] J. Ellis, J. L. Evans, F. Luo, K. A. Olive, and J. Zheng, Stop coannihilation in the CMSSM and SubGUT models, Eur. Phys. J. C **78**, 425 (2018).

[12] J. Ellis, J. L. Evans, F. Luo, N. Nagata, K. A. Olive, and P. Sandick, Beyond the CMSSM without an accelerator: Proton decay and direct dark matter detection, Eur. Phys. J. C **76**, 8 (2016).

[13] J. R. Ellis, K. A. Olive, and P. Sandick, Phenomenology of GUT-less supersymmetry breaking, J. High Energy Phys. 06 (2007) 079.

[14] J. R. Ellis, K. A. Olive, and P. Sandick, What if supersymmetry breaking appears below the GUT scale?, Phys. Lett. B **642**, 389 (2006).

[15] H. Georgi and S. L. Glashow, Unity of All Elementary Particle Forces, Phys. Rev. Lett. **32**, 438 (1974).

[16] N. Sakai, Naturalness in supersymmetric guts, Z. Phys. C **11**, 153 (1981).

[17] S. Dimopoulos and H. Georgi, Softly broken supersymmetry and SU(5), Nucl. Phys. **B193**, 150 (1981).

[18] M. C. Gonzalez-Garcia, M. Maltoni, and T. Schwetz, Updated fit to three neutrino mixing: Status of leptonic CP violation, J. High Energy Phys. 11 (2014) 052.

[19] I. Esteban, M. C. Gonzalez-Garcia, M. Maltoni, I. Martinez-Soler, and T. Schwetz, Updated fit to three neutrino mixing: Exploring the accelerator-reactor complementarity, J. High Energy Phys. 01 (2017) 087.

[20] F. Capozzi, E. Di Valentino, E. Lisi, A. Marrone, A. Melchiorri, and A. Palazzo, Global constraints on absolute neutrino masses and their ordering, Phys. Rev. D **95**, 096014 (2017).
[21] P. Minkowski, $\mu \to e\gamma$ at a rate of one out of 10^9 muon decays?, Phys. Lett. **67B**, 421 (1977).
[22] R. N. Mohapatra and G. Senjanovic, Neutrino Mass and Spontaneous Parity Violation, Phys. Rev. Lett. **44**, 912 (1980).
[23] M. Gell-Mann, P. Ramond, and R. Slansky, Complex spinors and unified theories, Conf. Proc. **C790927**, 315 (1979).
[24] J. Schechter and J. W. F. Valle, Neutrino masses in $SU(2) \times U(1)$ theories, Phys. Rev. D **22**, 2227 (1980).
[25] G. K. Leontaris, K. Tamvakis, and J. D. Vergados, Lepton and flavor violation in SUSY models, Phys. Lett. **171B**, 412 (1986).
[26] F. Borzumati and A. Masiero, Large Muon and Electron Number Violations in Supergravity Theories, Phys. Rev. Lett. **57**, 961 (1986).
[27] J. Hisano, T. Moroi, K. Tobe, and M. Yamaguchi, Lepton flavor violation via right-handed neutrino Yukawa couplings in supersymmetric standard model, Phys. Rev. D **53**, 2442 (1996).
[28] J. Hisano, T. Moroi, K. Tobe, M. Yamaguchi, and T. Yanagida, Lepton flavor violation in the supersymmetric standard model with seesaw induced neutrino masses, Phys. Lett. B **357**, 579 (1995).
[29] J. Hisano and D. Nomura, Solar and atmospheric neutrino oscillations and lepton flavor violation in supersymmetric models with the right-handed neutrinos, Phys. Rev. D **59**, 116005 (1999).
[30] L. Calibbi, A. Faccia, A. Masiero, and S. K. Vempati, Lepton flavour violation from SUSY-GUTs: Where do we stand for MEG, PRISM/PRIME and a super flavour factory, Phys. Rev. D **74**, 116002 (2006).
[31] S. Baek, T. Goto, Y. Okada, and K.-i. Okumura, Neutrino oscillation, SUSY GUT and B decay, Phys. Rev. D **63**, 051701 (2001).
[32] T. Moroi, CP violation in $B(d) \to \phi K(S)$ in SUSY GUT with right-handed neutrinos, Phys. Lett. B **493**, 366 (2000).
[33] N. Akama, Y. Kiyo, S. Komine, and T. Moroi, *CP* violation in kaon system in supersymmetric SU(5) model with seesaw induced neutrino masses, Phys. Rev. D **64**, 095012 (2001).
[34] T. Moroi, Effects of the right-handed neutrinos on Delta $S = 2$ and Delta $B = 2$ processes in supersymmetric SU(5) model, J. High Energy Phys. 03 (2000) 019.
[35] D. Chang, A. Masiero, and H. Murayama, Neutrino mixing and large *CP* violation in B physics, Phys. Rev. D **67**, 075013 (2003).
[36] J. Hisano and Y. Shimizu, GUT relation in neutrino induced flavor physics in SUSY SU(5) GUT, Phys. Lett. B **565**, 183 (2003).
[37] M. Ciuchini, A. Masiero, L. Silvestrini, S. K. Vempati, and O. Vives, Grand Unification of Quark and Lepton FCNCs, Phys. Rev. Lett. **92**, 071801 (2004).
[38] J. Hisano, M. Kakizaki, M. Nagai, and Y. Shimizu, Hadronic EDMs in SUSY SU(5) GUTs with right-handed neutrinos, Phys. Lett. B **604**, 216 (2004).
[39] A. J. Buras, M. Nagai, and P. Paradisi, Footprints of SUSY GUTs in Flavour Physics, J. High Energy Phys. 05 (2011) 005.
[40] T. Goto and T. Nihei, Effect of RRRR dimension five operator on the proton decay in the minimal SU(5) SUGRA GUT model, Phys. Rev. D **59**, 115009 (1999).
[41] H. Murayama and A. Pierce, Not even decoupling can save minimal supersymmetric SU(5), Phys. Rev. D **65**, 055009 (2002).
[42] T. Moroi, Sfermion masses in the supersymmetric SU(5) model with right-handed neutrinos, Phys. Lett. B **321**, 56 (1994).
[43] K. Kadota, K. A. Olive, and L. Velasco-Sevilla, A Sneutrino NLSP in the nu CMSSM, Phys. Rev. D **79**, 055018 (2009).
[44] K. Kadota and K. A. Olive, Heavy Right-Handed Neutrinos and Dark Matter in the nuCMSSM, Phys. Rev. D **80**, 095015 (2009).
[45] J. R. Ellis and M. K. Gaillard, Fermion masses and Higgs representations in SU(5), Phys. Lett. **88B**, 315 (1979).
[46] C. Panagiotakopoulos and Q. Shafi, Dimension Five Interactions, Fermion Masses and Higgs Mediated Proton Decay in SU(5), Phys. Rev. Lett. **52**, 2336 (1984).
[47] B. Bajc, P. F. Perez, and G. Senjanovic, Minimal supersymmetric SU(5) theory and proton decay: Where do we stand?, in *Beyond the desert: Accelerator, nonaccelerator and space approaches into the next millennium. Proceedings, 3rd International Conference on particle physics beyond the standard model, Oulu, Finland, 2002*, pp. 131–139, 2002, arXiv:hep-ph/0210374.
[48] C. Patrignani *et al.* (Particle Data Group), Review of particle physics, Chin. Phys. C **40**, 100001 (2016).
[49] S. Baek, T. Goto, Y. Okada, and K.-i. Okumura, Muon anomalous magnetic moment, lepton flavor violation, and flavor changing neutral current processes in SUSY GUT with right-handed neutrino, Phys. Rev. D **64**, 095001 (2001).
[50] F. Borzumati and T. Yamashita, Minimal supersymmetric SU(5) model with nonrenormalizable operators: Seesaw mechanism and violation of flavour and *CP*, Prog. Theor. Phys. **124**, 761 (2010).
[51] K. Tobe and J. D. Wells, Gravity assisted exact unification in minimal supersymmetric SU(5) and its gaugino mass spectrum, Phys. Lett. B **588**, 99 (2004).
[52] J. Hisano, H. Murayama, and T. Yanagida, Probing GUT Scale Mass Spectrum through Precision Measurements on the Weak Scale Parameters, Phys. Rev. Lett. **69**, 1014 (1992).
[53] L. J. Hall, J. D. Lykken, and S. Weinberg, Supergravity as the messenger of supersymmetry breaking, Phys. Rev. D **27**, 2359 (1983).
[54] J. Hisano, H. Murayama, and T. Goto, Threshold correction on gaugino masses at grand unification scale, Phys. Rev. D **49**, 1446 (1994).
[55] W. de Boer, R. Ehret, and D. I. Kazakov, Predictions of SUSY masses in the minimal supersymmetric grand unified theory, Z. Phys. C **67**, 647 (1995).
[56] M. Carena, J. R. Ellis, A. Pilaftsis, and C. E. M. Wagner, Higgs boson pole masses in the MSSM with explicit *CP* violation, Nucl. Phys. **B625**, 345 (2002).

[57] V. D. Barger, M. S. Berger, and P. Ohmann, The supersymmetric particle spectrum, Phys. Rev. D **49**, 4908 (1994).
[58] F. Gabbiani, E. Gabrielli, A. Masiero, and L. Silvestrini, A complete analysis of FCNC and *CP* constraints in general SUSY extensions of the standard model, Nucl. Phys. **B477**, 321 (1996).
[59] A. J. Buras, M. Misiak, and J. Urban, Two loop QCD anomalous dimensions of flavor changing four quark operators within and beyond the standard model, Nucl. Phys. **B586**, 397 (2000).
[60] S. Aoki *et al.*, Review of lattice results concerning low-energy particle physics, Eur. Phys. J. C **77**, 112 (2017).
[61] B. J. Choi *et al.* (SWME), Kaon BSM B-parameters using improved staggered fermions from $N_f = 2 + 1$ unquenched QCD, Phys. Rev. D **93**, 014511 (2016).
[62] Z. Bai, N. H. Christ, T. Izubuchi, C. T. Sachrajda, A. Soni, and J. Yu, $K_L - K_S$ Mass Difference from Lattice QCD, Phys. Rev. Lett. **113**, 112003 (2014).
[63] Z. Ligeti and F. Sala, A new look at the theory uncertainty of ϵ_K, J. High Energy Phys. 09 (2016) 083; Erratum, J. High Energy Phys. 02 (2017) 140(E).
[64] A. Crivellin, Z. Fabisiewicz, W. Materkowska, U. Nierste, S. Pokorski, and J. Rosiek, Lepton flavour violation in the MSSM: Exact diagonalization vs mass expansion, J. High Energy Phys. 06 (2018) 003.
[65] MEG, A. M. Baldini *et al.*, Search for the lepton flavour violating decay $\mu^+ \to e^+\gamma$ with the full dataset of the MEG experiment, Eur. Phys. J. C **76**, 434 (2016).
[66] ACME, J. Baron *et al.*, Methods, analysis, and the treatment of systematic errors for the electron electric dipole moment search in thorium monoxide, New J. Phys. **19**, 073029 (2017).
[67] G. F. Giudice and A. Romanino, Electric dipole moments in split supersymmetry, Phys. Lett. B **634**, 307 (2006).
[68] J. R. Ellis, J. S. Lee, and A. Pilaftsis, Electric dipole moments in the MSSM reloaded, J. High Energy Phys. 10 (2008) 049.
[69] Y. Li, S. Profumo, and M. Ramsey-Musolf, Higgs-Higgsino-Gaugino induced two loop electric dipole moments, Phys. Rev. D **78**, 075009 (2008).
[70] J. Hisano, M. Nagai, and P. Paradisi, Flavor effects on the electric dipole moments in supersymmetric theories: A beyond leading order analysis, Phys. Rev. D **80**, 095014 (2009).
[71] G. Degrassi, E. Franco, S. Marchetti, and L. Silvestrini, QCD corrections to the electric dipole moment of the neutron in the MSSM, J. High Energy Phys. 11 (2005) 044.
[72] J. Hisano, J. Y. Lee, N. Nagata, and Y. Shimizu, Reevaluation of neutron electric dipole moment with QCD sum rules, Phys. Rev. D **85**, 114044 (2012).
[73] J. Hisano, D. Kobayashi, W. Kuramoto, and T. Kuwahara, Nucleon electric dipole moments in high-scale supersymmetric models, J. High Energy Phys. 11 (2015) 085.
[74] K. Abe *et al.* (Super-Kamiokande Collaboration), Search for proton decay via $p \to \nu K^+$ using 260kilotonyear data of Super-Kamiokande, Phys. Rev. D **90**, 072005 (2014).
[75] V. Takhistov Super-Kamiokande Collaboration, Review of Nucleon Decay Searches at Super-Kamiokande, in *Proceedings, 51st Rencontres de Moriond on Electroweak Interactions and Unified Theories, La Thuile, Italy, 2016* (2016), pp. 437–444.
[76] J. Hisano, H. Murayama, and T. Yanagida, Nucleon decay in the minimal supersymmetric SU(5) grand unification, Nucl. Phys. **B402**, 46 (1993).
[77] J. Hisano, D. Kobayashi, T. Kuwahara, and N. Nagata, Decoupling can revive minimal supersymmetric SU(5), J. High Energy Phys. 07 (2013) 038.
[78] N. Nagata and S. Shirai, Sfermion flavor and proton decay in high-scale supersymmetry, J. High Energy Phys. 03 (2014) 049.
[79] J. L. Evans, N. Nagata, and K. A. Olive, SU(5) grand unification in pure gravity mediation, Phys. Rev. D **91**, 055027 (2015).
[80] C. Munoz, Enhancement factors for supersymmetric proton decay in SU(5) and SO(10) with superfield techniques, Phys. Lett. **177B**, 55 (1986).
[81] L. F. Abbott and M. B. Wise, The effective Hamiltonian for nucleon decay, Phys. Rev. D **22**, 2208 (1980).
[82] T. Nihei and J. Arafune, The two loop long range effect on the proton decay effective Lagrangian, Prog. Theor. Phys. **93**, 665 (1995).
[83] Y. Aoki, T. Izubuchi, E. Shintani, and A. Soni, Improved lattice computation of proton decay matrix elements, Phys. Rev. D **96**, 014506 (2017).
[84] A. M. Baldini *et al.* (MEG II Collaboration), The design of the MEG II experiment, Eur. Phys. J. C **78**, 380 (2018).
[85] J. Ellis, K. A. Olive, and J. Zheng, The extent of the stop coannihilation strip, Eur. Phys. J. C **74**, 2947 (2014).
[86] K. Abe *et al.*, Letter of intent: The hyper-Kamiokande experiment-detector design and physics potential, arXiv:1109.3262.
[87] S. A. R. Ellis and B. Zheng, Reaching for squarks and gauginos at a 100 TeV $p - p$ collider, Phys. Rev. D **92**, 075034 (2015).